

Isolation and biological activities of naturally occurring apocarotenoid bixin

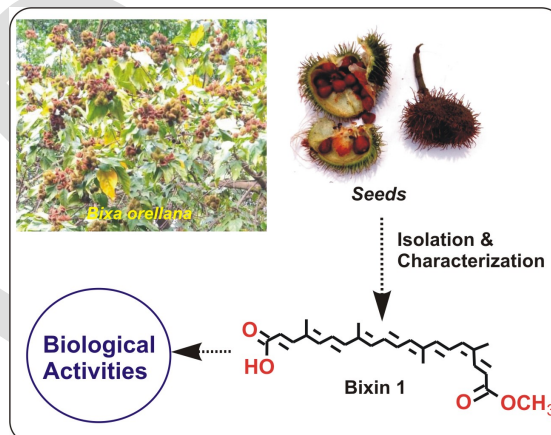
Soumen Patra, Sukhendu Kar, Braja Gopal Bag*

Department of Chemistry and Chemical Technology, Vidyasagar University, Midnapore 721102

Email: brajagb@gmail.com

Received: October 16, 2021 | Accepted: December 21, 2021 | Published online: December 28, 2021

The naturally occurring apo-carotenoid bixin is obtained from annatto (*Bixa orellana*). It is unique among the natural carotenoids through its water solubility and easily extractability from the seed coat of *Bixa orellana*. Bixin is (2E,4E,6E,8E,10E,12E,14E,16Z,18E)-20-methoxy-4,8,13,17-tetramethyl-20-oxico-2,4,6,8,10,12,14,16,18-nonaenoic acid, an apo-carotenoid which is a terpenoid compound derived from the oxidative cleavage of carotenoids. Several biological activities of bixin has been reported earlier such as selective antimyeloma effects of cis-bixin, antinociceptive and anti-inflammatory effects, antioxidant action against cis-platine induced chromosome in rats, hypoglycemic effect in alloxan-induced diabetic rats, allodynia, anxious and depressive-like behaviors, targeting NRF2 for improved skin barrier function and photoprotection, antiatherogenic effect in hypercholesterolemic rabbits, triggering apoptosis of cancer cells, immunomodulatory role in dogs, sensitization of human melanoma cells to dacarbazine-induced apoptosis, sensitization of human lung cancer and cervical cancer cell to cisplatin in vitro, anti-SARS-CoV-2 activity, antibacterial activity of cis-bixin conjugated silver nanoparticles, protective effect on carbon tetrachloride-induced hepatotoxicity in rats, bixin/crocin nanoparticles on quality and shelf life improvement of cheddar cheese etc. In this review, the biological properties of bixin has been discussed. A practical method for the isolation of bixin 1 from the seed coat of *Bixa orellana* commonly known as "Sinduri" (in Bengali) and its characterization has also been reported.



Keywords: *Bixa orellana* (Sinduri), medicinal plants, antioxidant, anti-inflammatory, immunomodulatory, antimyeloma

1. Introduction

From the plants we can have large quantities of renewable chemicals like polyphenols, flavonoids, terpenoids, fatty acids, xanthanoids, carotenoids, alkaloids etc.^{1,2,3,4,5,6,7,8,9,10,11,12,13,14,15,16,17} Triterpenoids having multifold isoprene units (C₅) are major secondary plant metabolites, bio-synthesized in plants via complex enzymatic pathway from its biosynthetic precursor squalene or oxidosqualene. Bixin is (2E,4E,6E,8E,10E,12E,14E,16Z,18E)-20-methoxy-4,8,13,17-tetramethyl-20-oxico-2,4,6,8,10,12,14,16,18-nonaenoic acid, an apo-carotenoid which is a terpenoid compound derived from the oxidative cleavage of carotenoids.¹⁸ As the petroleum based chemicals are depleting very fast, scientists are focused on renewable plant based chemicals. Since the last few decades triterpenoids have achieved tremendous research interest in various fields of science due to their nontoxic nature, nanometric lengths, natural availability, amphiphilic character, bio-compatibility

etc. Bixin has various medicinal activities such as selective antimyeloma effects of cis-bixin, antinociceptive and anti-inflammatory effects, antioxidant action against cis-platine induced chromosome in rats, hypoglycemic effect in alloxan-induced diabetic rats, allodynia, anxious and depressive-like behaviors, targeting NRF2 for improved skin barrier function and photoprotection, antiatherogenic effect in hypercholesterolemic rabbits, triggering apoptosis of cancer cells, immunomodulatory role in dogs, anti-SARS-CoV-2 activity, antibacterial activity of cis-bixin conjugated silver nanoparticles, protective effect on carbon tetrachloride-induced hepatotoxicity in rats, etc. which have been discussed in this article. Isolation procedure of bixin from the seed coat of *Bixa orellana* fruit and its characterization through ¹H-NMR, ¹³C-NMR, DEPT 90, DEPT 135, FTIR and HRMS spectroscopy have also been described.

2. Biological activity of bixin

Bixin has been shown to exhibit various biological activities which are shown schematically in Figure 1. Those

biological activities have been discussed in the following sections (sections 2.1-2.13).

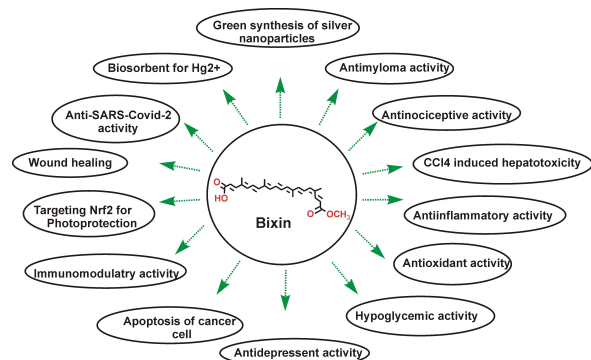


Figure 1: Schematic presentation of biological activities of Bixin

2.1 Selective antimyeloma effects of cis-bixin

Cis-bixin shows antimyeloma effects which was studied under ex-vivo assays in the myeloma samples of patient and non-cross resistance in highly drug-resistant myeloma cell lines. Moreover, cis-bixin shows its cytotoxic effects through cellular ROS imposition, mediated through thioredoxin/thioredoxin reductase inhibition in the redox pathway (Figure- 2).¹⁹

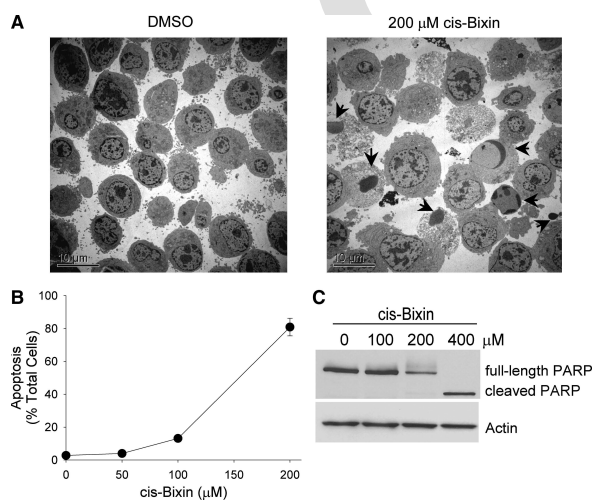


Figure 2: Cis-bixin-induced cytotoxicity in myeloma cells is associated with apoptosis. (A) Electron microscopic images (x2,500) of OCI-MY-5 myeloma cells treated with DMSO diluent or 200 mM cis-bixin, demonstrating induction of morphologic apoptosis (arrows). (B) Concentration-dependence of apoptosis induction by cis-bixin in OCI-MY-5 myeloma cells. Apoptosis was assessed with Hoechst 33258 nuclear staining after 24-h exposures to indicated cis-bixin concentrations; error bars indicate +1 standard deviation. (C) Cis bixin induces PARP cleavage in OCI-MY-5 cells (24-h drug exposures). (Adapted from Ref.19)

2.2 Antinociceptive and anti-inflammatory

Bixin shows both the antinociceptive and anti-inflammatory activities. The anti-inflammatory activity of bixin was performed by its oral administration in the proportion of 15 or 30 mg/kg in carrageenan induced paw edema as well as myeloperoxidase (MPO) activity in male Wistar rats. The antinociceptive effect of bixin was carried out at same doses in both the formalin and hot plate tests in rats and in the Swiss albino male mice at dose proportion of 27 or 53 mg/kg through acetic acid-induced writhing test. Both the doses of bixin remarkably decreased the flinches number in both phases of formalin test and number of the acetic acid-induced writhings without changing the open field locomotor performance test.²⁰

2.3 Antioxidant activity

Bixin shows antioxidant activity through cisplatin-induced oxidative stress in Wistar rats through three markers of oxidative damage: chromosome aberrations, glutathione depletion and lipid peroxidation.²¹

2.4 Hypoglycemic activity

Bixin shows hypoglycemic activity both in vivo as well as in silico study. Oral intake of Bixin (10mg/kg) remarkably decreased the glucose level in alloxan-induced diabetic rats. Bixin also shows in silico selectivity on peroxisome proliferator-activated receptors (PPARs), particularly by the peroxisome proliferator-activated receptor gamma (PPAR γ), which supports the hypoglycemic activity of Bixin.²²

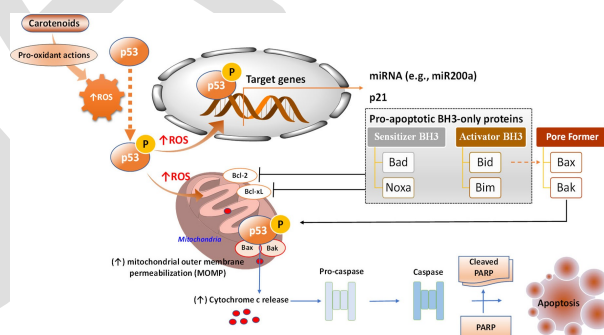


Figure 3: Mechanisms of the carotenoids-mediated p53-induced apoptosis of cancer cells. Bcl-2: B-cell lymphoma 2; Bad: Bcl-2-associated agonist of cell death; Bak: Bcl-2 homologous antagonist/killer; Bax: Bcl-2-associated X protein; Bcl-xL: Bcl-extra-large; Bid: BH3 interacting-domain death agonist; Bim: Bcl-2-like protein 11; Noxa: Latin for damage, also known as phorbol-12-myristate-13-acetate-induced protein PMAIP1; PARP: poly (ADP-ribose) polymerase. (Adapted from Ref.24)

2.5 Anxious and depressive-like behaviors

Bixin could be used as traditional medicine to treat diabetes and could be recognized through its antioxidant profile. The whole experiment was carried out on Streptozotocin-induced diabetic rats for 17 days. The result showed that bixin may represent an alternative for the treatment of comorbidities associated with diabetes, counteracting oxidative stress and plasma hemoglobin (HbA1).²³

2.6 Triggering apoptosis of cancer cells

Bixin could increase the ROS levels in the melanoma A2058 cells of human. Treatment of bixin with dacarbazine causes gradually greater toxicity (IC50 of 31.85 μM) comprises to the individual treatments (IC50 of 40.53 μM for bixin which is much much greater than 100 μM for dacarbazine), showing the advantagel of using this carotenoid as the anti-cancer drugs in the treatment of cancers (Figure 3).²⁴

2.7 Immunomodulatory activity

Chew and coworkers have studies the uptake of bixin by plasma, lipoproteins, and leukocytes in domestic dogs and examined the immunoprotective properties. They found that bixin was readily absorbed in a dose-dependent manner in blood following oral administration. Later it was taken up by leukocytes, where it was primarily distributed to mitochondria along with other subcellular organelles. Stimulation of immune response was also observed with cell-mediated responses in dogs.²⁵

2.8 Targeting NRF2 for photoprotection

The bixin is used as canonical activator for the NRF2-dependent cytoprotective response in human skin keratinocytes; that systemic administration of bixin activates NRF2 with protective effects against solar UV-induced skin damage; and that bixin-induced suppression of photodamage is observable in *Nrf2^{+/+}* but not in *Nrf2^{-/-}* SKH-1 mice confirming the NRF2-dependence of bixin-induced antioxidant and anti-inflammatory effects (Figure- 4 & 5).²⁶

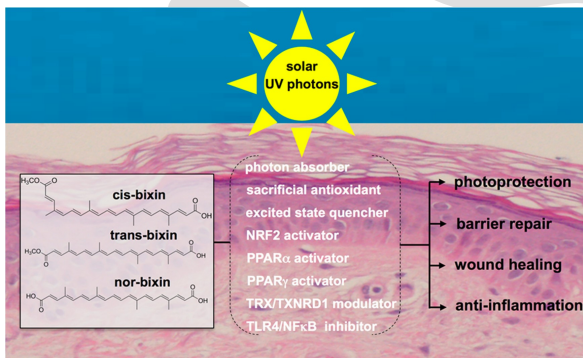


Figure 4: Bixin for improved skin barrier function and photoprotection. Based on pleiotropic activities including direct chemical and NRF2-dependent antioxidant modulation, cis-bixin and its physiologically relevant derivatives trans-bixin and nor-bixin enhance skin barrier structure and function with photoprotective and potentially photochemopreventive efficacy; thioredoxin (TRX), thioredoxin reductase 1 (TXNRD1) (Adapted from Ref.26)

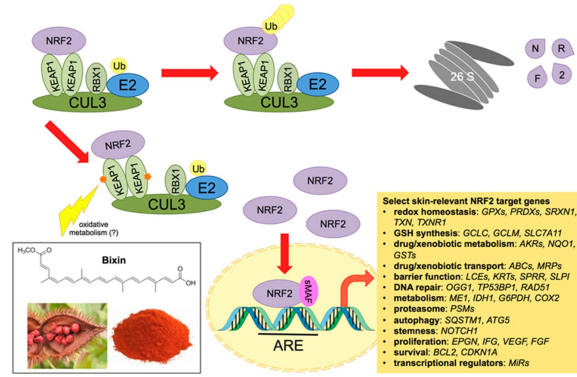


Figure 5: The nuclear factor-E2-related factor 2 (NRF2) pathway with a focus on skin barrier function and environmental stress protection. The transcription factor NRF2 binds to Kelch-associated protein 1 (KEAP1), the substrate adaptor protein for the cullin 3-RING box protein 1 (CUL3-RBX1) E3 ubiquitin ligase complex. Under basal conditions, NRF2 is ubiquitinated and degraded by the 26S proteasome. Upon modification of reactive cysteines in KEAP1 by reactive oxygen species (ROS) and electrophiles (including bixin), NRF2 is no longer ubiquitinated. This allows for newly synthesized NRF2 to accumulate, translocate to the nucleus, and activate the transcription of antioxidant response element (ARE)-containing target genes by dimerizing with small MAF (sMAF) proteins. Select skin-relevant NRF2 target genes are displayed according to the cellular function they perform. GPXs, glutathione peroxidases; PRDXs, peroxiredoxins; SRXN1, sulfiredoxin 1; TXN, thioredoxin; TXNR1, thioredoxin reductase 1; GCLC, glutamate cysteine ligase, catalytic subunit; GCLM, glutamate cysteine ligase, modifier subunit; SLC7A11, glutamate/cystine antiporter (xCT); AKRs, aldoketoreductases; NQO1, NAD(P)H:quinone oxidoreductase 1; GSTs, glutathione S-transferases; ABCs, ATP-binding cassette family proteins; MRPs, multidrug resistance-associated proteins; LCEs, late cornified envelope family members; KRTs, keratins; SPRR, small proline rich proteins; OGG1, 8-oxo-guanine glycosylase; TP53BP1, p53 binding protein 1; RAD51, DNA repair protein RAD51 homolog 1; ME1, malic enzyme; IDH1, isocitrate dehydrogenase 1; G6PDH, glucose-6-phosphate dehydrogenase; COX2, cytochrome c oxidase subunit 2; PSM, proteasome subunit proteins; SQSTM1, sequestosome 1 (p62); ATG5, autophagy-related gene 5; NOTCH1, Notch homolog 1, translocation-associated; EPGN, epigen; IGF, insulin-like growth factor; VEGF, vascular endothelial growth factor; FGF, fibroblast growth factor; BCL2, B cell lymphoma 2; CDKN1A, cyclin depende. (Adapted from Ref.26)

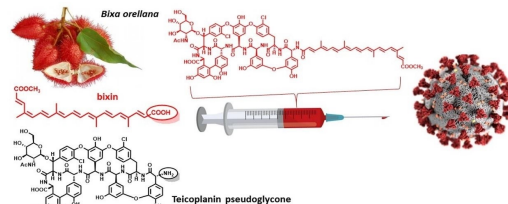


Figure 6: Schematic representation of bixin showing anti-SARS-CoV-2 activity. (Adapted from Ref.27)

2.9 Anti-SARS-CoV-2 activity

The bixin shows tremendous anti-SARS-CoV-2 activity as it is very cheap and extensively used in food additive as red colourant. The anti-SARS-CoV-2 activity was tested in

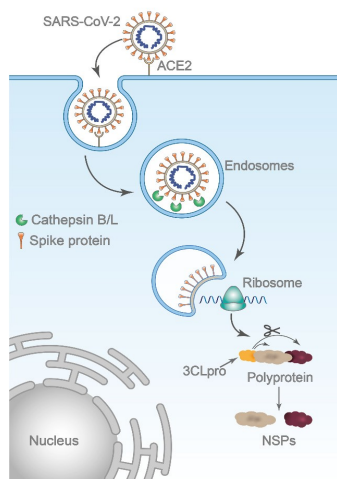


Figure 7: Schematic representation of SARS-CoV-2 entry by the endosomal route. After binding to its host receptor angiotensin-converting enzyme 2 (ACE2), the virus is internalized via endocytosis. The low pH within the endosome activates Cat L, which in turn triggers membrane fusion by proteolytic cleavage of the S protein. Upon membrane fusion, viral genomic RNA is released in the cytoplasm and initiates translation of polyproteins, which is, subsequently, cleaved into nonstructural proteins (NSPs) by viral main protease 3CLpro. Several NSPs constitute the replicase-transcriptase complex essential for viral replication. (Adapted from Ref.27)

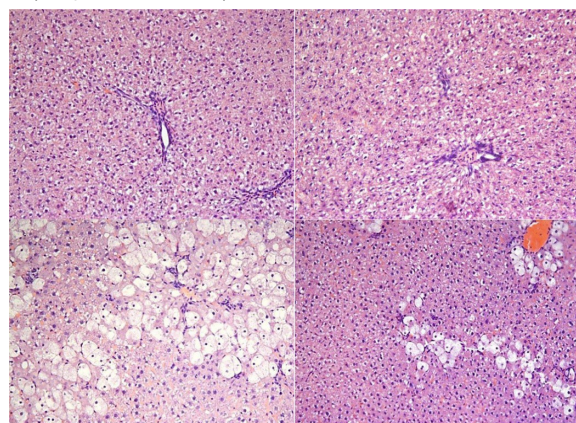


Figure 8: The effects of bixin on CCl₄-induced liver damage in rat. (A) liver of control group showing intact liver structures; (B) liver of bixin group, showing normal structure; (C) liver of CCl₄ group, showing hepatocytes necrosis (arrow head), hydropic degeneration (arrow) and infiltration of inflammatory cells (dashed arrow); and (D) liver of CCl₄ + bixin showing prevented damage. H&E, original magnification 200 ×. (Adapted from Ref.29)

Vero E6 cells in viability assay of cells and viral RNA quantitative PCR which confirms their inhibitory activity in micromolar quantity against viral replication. Bixinoids also

shows its potential in the inhibition of Zika Virus by using molecular simulations (Figure- 6 & 7).²⁷

2.10 Green synthesis of silver nanoparticles

Poornima et al have reported the green synthesis of *Bixa orellana* L. leaf extract and seed coat extract conjugated AgNPs using the leaf and the dye extract (nor-bixin) under sunlight. The size of the nanoparticles were 30-100 nm 10-80 nm respectively. Both the conjugated AgNPs showed promising antibacterial activity against both gram positive bacteria *Staphylococcus aureus* and gram negative bacteria *Escherichia coli*.²⁸

2.11 CCl₄-induced hepatotoxicity inhibition in rats

The carotenoid bixin is having antioxidant property which can protect cells and tissues from deleterious effects of free radicals. The bixin shows protective effect for liver damage caused by carbon tetrachloride (CCl₄) in rats (Figure 8).²⁹

2.12 Wound healing

The bixin-loaded polycaprolactone (PCL) nanofibers could act as wound healing controlled delivery system. Bixin

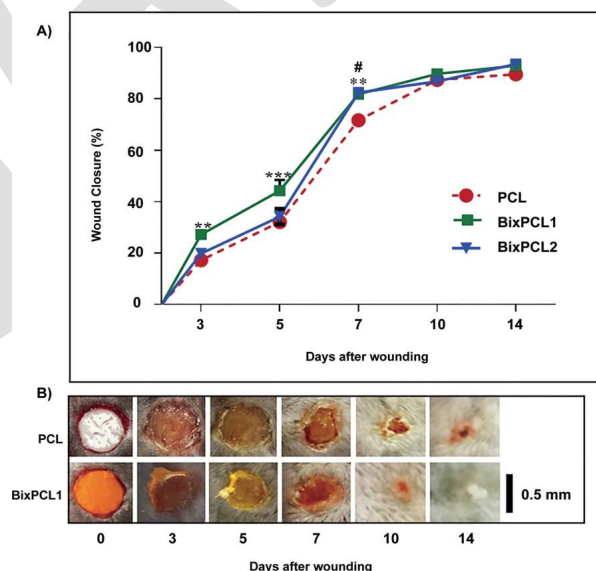


Figure 9: Influence of Bix-PCL1 nanofibers on wound closure after an excisional skin injury. In this experimental model, the skin wound healing occurs from the wound margins. (A) Time course of wound closure in diabetic mice. Values were represented as means (SEM) from groups of 10 animals each. *** $p < 0.05$ and # $p < 0.001$ versus control group (Two-way ANOVA). (B) Representative macroscopic pictures of wound closure area treated with PCL or BixPCL1 nanofibers. (Adapted from Ref.30)

(Bix) has a great influence on PCL nanofiber. The investigation of Bix-PCL1(2.5% w/w bix) and Bix-PCL2 (12.5% w/w bix) formation was performed through electrical conductivity, attenuated total reflectance infrared

spectroscopy, XRD, thermal analysis, and SEM. From the excisional wound model in induced diabetic mice, released bixin low concentration from Bix-PCL loaded nanofibers shows biological activity of bixin and has efficient accelerating wound healing and reducing the scar tissue area as compared to pure PCL nanofibers. Thus, bixin-loaded soft PCL nanofibers have efficient use in wound dressing (Figure 9).³⁰

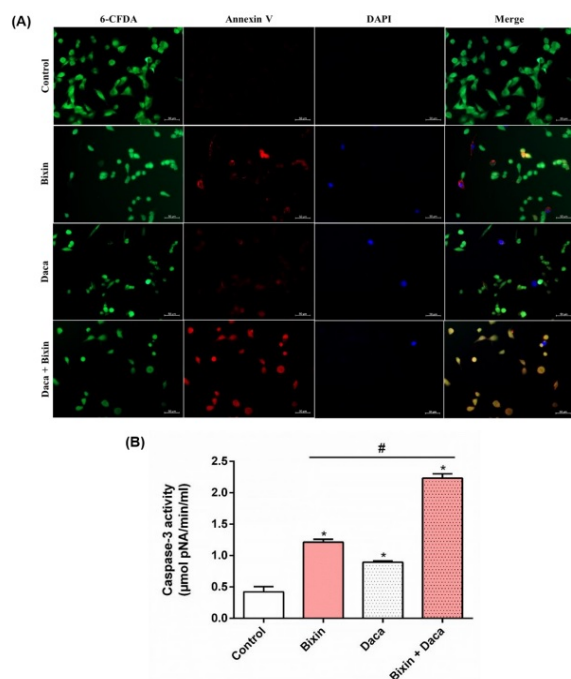


Figure 10: Bixin improves pro-apoptotic effect of dacarbazine. Fluorescent micrographs show A2058 cells after Annexin V (red), 6-CFDA (green) and DAPI (blue) staining (A). Caspase-3 activity was evaluated after 72h of treatment (B). Cells were treated with bixin 50 µM, dacarbazine 50 µM (daca) or combined therapy (bixin + daca). Data are expressed as mean ± SEM, *p<0.05 (vs. control group) and #p<0.05 (vs. dacarbazine), according to ANOVA one-way followed by Tukey's post-test. (Adapted from Ref.32)

2.12 Bixin as biosorbent for Hg²⁺ removal from aqueous solutions

Bixin is used as potential biosorbent in aqueous solutions of Hg²⁺. In a thin film having inert support, the bixin has been used through drop-coating method. The thin film has been characterised through SEM, TGA-DTG and ATR-FTIR techniques. The thin bixin film has been used in samples having spiked environment, showing 86 % removal of Hg²⁺. This results confirming the efficient removal of mercury from several aqueous systems for bixin film. This opens a new mode of biosorbent based on apocarotenoids, that are low cost, easily obtainable, sustainable, and nontoxic in nature.³¹

2.13 Dacarbazine-induced apoptosis through ROS-mediated cytotoxicity of Bixin

Bixin when sensitized to human melanoma cells (A2058) to dacarbazine treatment, an anticancer agent clinically used for the therapy of metastatic melanoma. Bixin (Z-bixin) was

evaluated on A2058 cells expressing the oncogenic BRAF VE600 mutation and resistant to dacarbazine treatment. Bixin promoted growth inhibition, reduced cell migration, induced apoptosis and cell cycle arrest in the G2/M phase. When associated with dacarbazine, bixin restored the sensitivity of A2058 cells to chemotherapy, enhancing its antiproliferative, anti-migratory and pro-apoptotic effects (Figure- 10, 11, 12).³²

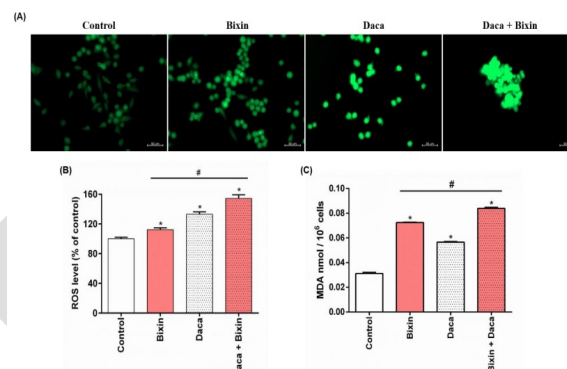


Figure 11: Effect of bixin 50 µM, dacarbazine 50 µM (daca), and combined therapy (bixin + daca) on qualitative (A) and quantitative (B) ROS generation and MDA production (C) in A2058 cells. Data are expressed as mean ± SEM, *p<0.05 (vs. control group) and #p<0.05 (vs. bixin and dacarbazine groups), according to ANOVA one-way followed by Tukey's post-test. (Adapted from Ref.32).

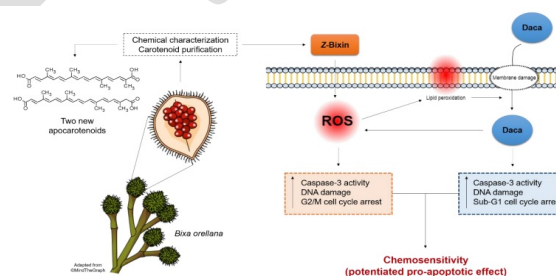


Figure 12: Graphical representation of the chemoselectivity of Z-bixin. (Adapted from Ref.32)

3. Source of bixin

Bixin can only be obtained from seed coat of annatto (*Bixa orellana*) plant through solvent extraction procedure. *Bixa orellana*, an evergreen shrub, usually known as annatto, lipstick tree or sinduri plant is a small tree from which beautiful star-shaped pink flowers and rambutan-like scarlet fruit are obtained. The red-orange colour pigment was obtained from the pulp can be used as food colorant as well as for commercial dye. The height of the plant is usually 6 - 20 feet and it can survive up to 50 years. Lipstick tree has been widely cultivated in India for many centuries to get the yellow-orange dye obtained from its seeds for safe coloring agent for foods. Near about 50 seeds may be grown inside of the pod. Based on color of the flowers, the seedpod may be either green or red but the seeds have the same coating in both.³³ These seeds are processed to obtain the orange-yellow pigments, bixin and norbixin (carotenoids), as dye for food, cosmetic and soap industries.³⁴ This dye may also be

used for coloring the cheddar cheese and for coloring of rice.³⁵ The dried pulp of the fruit has only been used for such purposes.

3. Experimental Section

3.1 General experimental procedures

All the solvents of commercial grade was used for the extraction, isolation and purification were distilled freshly before use. Several spectral characterizations like ¹H and ¹³C NMR spectra were recorded at 400 MHz and 100 MHz respectively, on a Bruker NMR spectrometer. HRMS was obtained with Agilent 6230B TOF. FTIR was performed with Perkin Elmer spectra.

3.2 Collection of plant materials

The fresh green coloured fruits of *Bixa Orellana* (sinduri) were collected from 'Elliot park' in Kolkata, West Bengal, India, in January 2019.

3.3 Isolation and Purification of Bixin

Sun dried seeds (100 g) of *Bixa orellana* (sinduri) was extracted ethyl acetate (150 mL X 5) by stirring magnetically at room temperature for 5 hours and filtered (filter paper). The volatiles were under reduced pressure to obtain pink red coloured crude residue (4.93 g). From the 4.93 g of crude we take 1.823 g to purify by successive column chromatography (2 times, silica gel, 100–200 mesh, 0.9 × 17 cm) using 30% ethyl acetate/dichloromethane as the eluent. The product appeared as a pink-red solid (124 mg, 6.80% yield) (scheme 1). R_f = 0.606 (30% ethyl acetate/dichloromethane). MP = 215–217°C (Figure- 13).

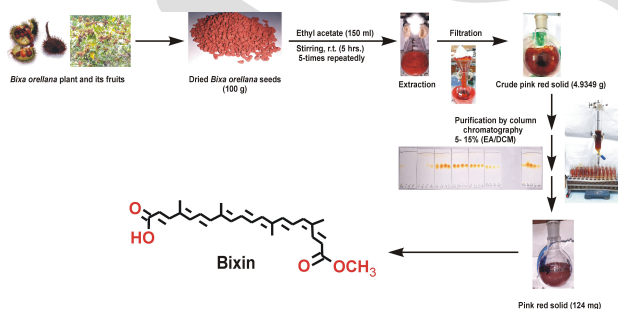


Figure 13: Schematic presentation of isolation of bixin from the seed coat of *Bixa orellana* (Scheme 1)

3.3 Structural Characterization

The compound was characterized via different spectroscopic techniques like ¹H NMR, ¹³C NMR, DEPT 90, DEPT 135, HRMS, and FTIR. Bixin 1 having molecular formula C₂₅H₃₀O₄ has been established by HRMS. ¹H NMR (400 MHz, CDCl₃): δ 8.007 (1H, d), δ 7.501 (1H, d), δ 6.890 (1H, dd), δ 6.732-6.695 (2H, dd), δ 6.659-6.540 (3H, m), δ 6.452-6.414 (1H, d), δ 6.378-6.357 (2H, d), δ 6.357-6.331 (1H, d), δ 5.952-5.879 (2H, dd), δ 3.793 (3H, s), δ 2.030 (3H, s), δ 2.011 (3H, s), δ 1.982 (6H, s) ppm (Figure 14a). From ¹H NMR spectrum it is evident that in the molecule there are four “-CH₃” groups having δ values 2.030, 2.001 and 1.982 ppm respectively and “-OCH₃” groups having the δ value 3.793. ¹³C NMR (CDCl₃, 100 MHz): δ 171.67 (C1), 168.01

(C20), 151.08 (C3), 142.38 (C18), 140.50 (C17), 140.39 (C8), 137.95 (C4), 137.14 (C13), 136.56 (C14), 135.22 (C7), 134.21 (C9), 133.57 (C5), 131.60 (C10), 131.46 (C6), 130.73 (C16), 130.73 (C12), 124.21 (C19), 123.38 (C2), 117.53 (C11), 115.05 (C15), 51.615 (C20-OCH₃), 20.568 (C17-CH₃), 13.012 (C4-CH₃), 12.774 (C8-CH₃), 12.637 (C13-CH₃) ppm (Figure 14b). The ¹³C spectrum clearly indicated the presence of 25 carbon atoms in the molecule.^{36,37,38} To further

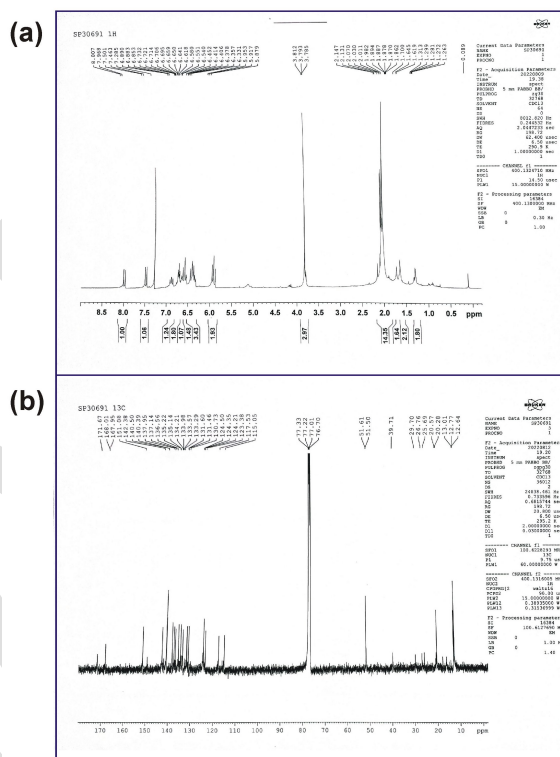


Figure 14a: ¹H NMR and 14b: ¹³C NMR spectroscopy of bixin 1

elucidate the structure of the molecule, DEPT 90 and DEPT 135 experiments were carried out. DEPT 90 (CDCl₃, 100 MHz): δ 151.09, 142.39, 140.51, 140.41, 137.99, 135.23, 134.24, 131.46, 130.73, 130.73, 124.21, 123.38, 117.50, 115.04. DEPT 90 shows the presence of 14 ‘-CH’s in the

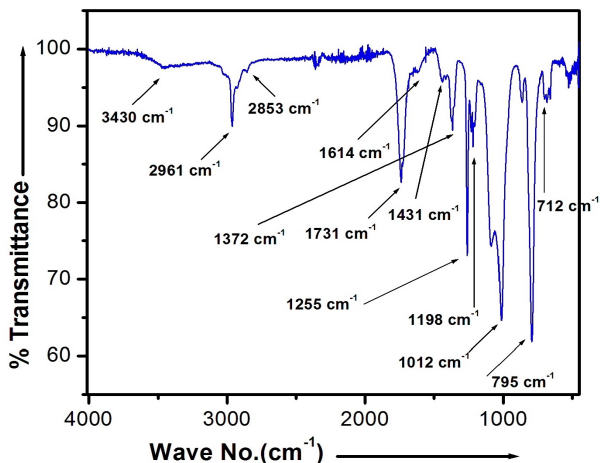


Figure 18 · FTIR spectrum of bixin 1

molecule. (Figure 15b); DEPT 135 (CDCl₃, 100 MHz): δ 151.08, 142.39, 140.52, 140.41, 137.99, 135.23, 134.24, 131.46, 130.73, 130.73, 124.22, 123.38, 117.51, 115.05, 20.32, 13.03, 12.80, 12.66 (Figure 7b). DEPT 135 indicated the presence of 4 '-CH₃' groups along with the presence of 14 '-CH's in the molecule as evident from DEPT 90 and ¹³C NMR. FTIR (ν, cm⁻¹): We performed the FTIR spectroscopy and following bands were obtained in the bixin molecule

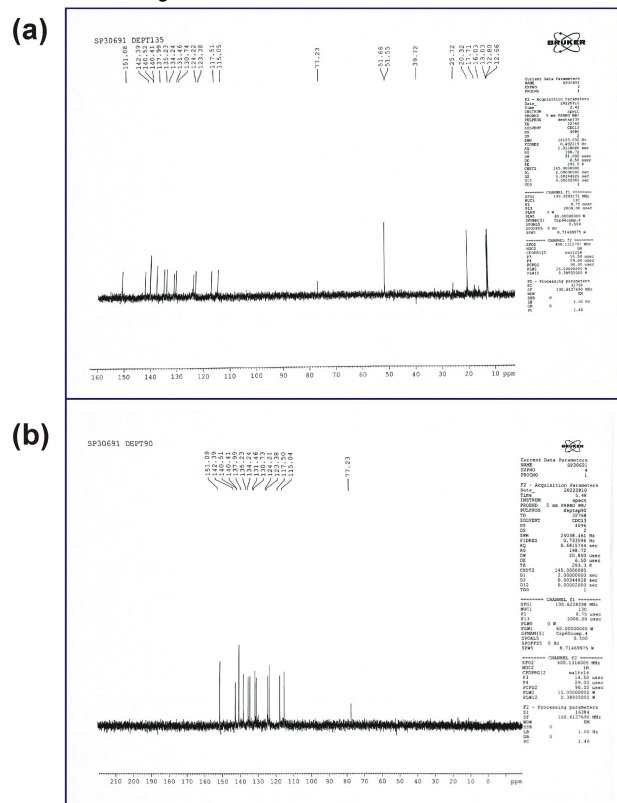


Figure 15a: DEPT 135 and 15b: DEPT 90 of bixin 1

(Figure- 18). We have band at 3430 cm⁻¹ indicating the '-O-H' stretching vibration, bands at 2961 cm⁻¹ and 2853 cm⁻¹ indicating the 'H-C-H' bending vibration, bands at 1731 cm⁻¹ indicating the 'C=O' ester group, band at 1614 cm⁻¹ indicating the '-O-H' bending vibration, band at 1431 cm⁻¹ indicating the alkene C=C stretching, band at 1372 cm⁻¹ indicating the C-H bending of methyl groups, band at 1255 cm⁻¹ indicating the 'C=O' stretching, band at 1198 cm⁻¹ symmetric and

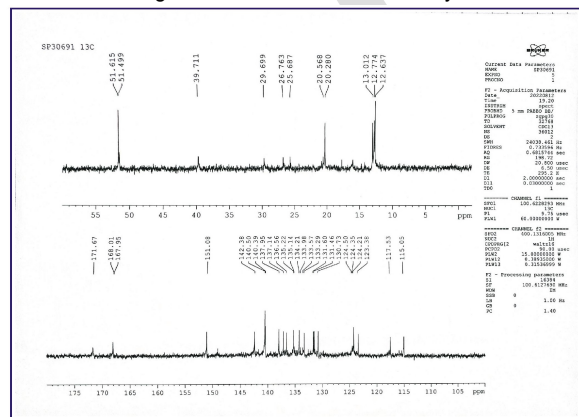


Figure 16: Expand ¹³C NMR of bixin 1

asymmetric vibrations of the C-O-C ester group, and the band at 712 cm⁻¹ indicating the methylene rocking vibration of cis carotenoid.³⁹ The NMR data obtained for the compound are comparable to those previously reported in the literature.

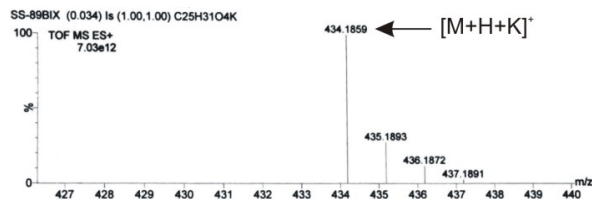


Figure 17: HRMS spectroscopy of bixin 1

HRMS: m/z calculated for (M+H+K)⁺ = 434.1859; obtained 434.1859 (Figure- 17).

4. Conclusion and outlook

In this article we have reviewed extraction, purification and various biological activities of bixin. The detail structural analysis of bixin was carried out by us by various spectroscopic techniques such as ¹H NMR, ¹³C NMR, DEPT-135, FTIR and HRMS. The molecule has a lipophilic aliphatic extended conjugated structure with one carboxyl (-COOH) group located at one extreme end of the molecule preferring it as a molecular functional nano-entity to design for advanced functional materials and nano-biotechnology.

5. Acknowledgement

BGB thanks CSIR New Delhi, DST-FIST New Delhi and Vidyasagar University for financial support and infrastructural facilities.

References

1. A. Eschenmoser, L. Ruzicka, O. Jeger, D. Arigoni, *Helv. Chim. Acta.* **1955**, *38*, 1890-1904.
2. A. Eschenmoser, D. Arigoni, *Helv. Chim. Acta.* **2005**, *88*, 3011-3050.
3. B. G. Bag, A. C. Barai, S. N. Hasan, S. K. Panja, S. Ghorai, S. Patra, *Pure Appl. Chem.* **2020**, 567.
4. B. G. Bag, S. Das, S. N. Hasan, A. C. Barai, S. Ghorai, S. K. Panja, C. Garai, S. Santra, *Prayogik Rasayan.* **2018**, *2*, 1-23
5. B. G. Bag, C. Garai, R. Majumdar, M. Laguerre, *Struct. Chem.* **2012**, *23*, 393-398.
6. B. G. Bag, A. C. Barai, S. N. Hasan, S. Das, C. Garai, S. Ghorai, S. K. Panja, *Prayogik Rasayan.* **2017**, *1*, 61-68.
7. B. G. Bag, R. Majumdar, *Chem. Rec.* **2017**, *17*, 841-873.
8. B. G. Bag, R. Majumdar, *RSC Adv.* **2012**, *2*, 8623-8626.
9. D. Tungmunthum, A. Thongboonyou, A. Pholboon, A. Yongsabai, *Medicines.* **2018**, *5*, 93.
10. B. G. Bag, K. Paul, *Asian J. Org. Chem.* **2012**, *1*, 150-154.
11. B. G. Bag, S. S. Dash, *Langmuir.* **2015**, *31*, 13664-13672.

12. B. G. Bag, S. Das, S. N. Hasan, A. C. Barai, *RSC Adv.* **2017**, 7, 18136–18143.
13. B. G. Bag, C. Garai, S. Ghorai, *RSC Adv.* **2019**, 9, 15190–15195.
14. S. Ghorai, B. G. Bag, *ACS Omega.* **2021**, 6, 31, 20560–20568.
15. S. K. Panja, B. G. Bag, *ACS Omega.* **2020**, 5, 47, 30488–30494.
16. S. Ghorai, B. G. Bag, *Chemistry Select.* **2020**, 5, 47, 15032–15038.
17. S. K. Panja, S. Patra, B. G. Bag, *RSC Adv.* **2021**, 11, 33500–33510.
18. R. R. Madrid, M. A. Espinosa, Y. C. Conejo, L. E. G. Caligaris, *Front. Plant Sci.* **2016**, <https://doi.org/10.3389/fpls.2016.01406>.
19. J. D. Tibodeau, C. R. Isham, K. C. Bible, *Antioxidants & Redox Signaling.* **2010**, 13, 987–997.
20. S. D. G. Pacheco, A. T. Gasparin, C. H. A. Jesus, B. B. Sotomaior, A. C. S. S. B. Ventura, D. D. B. Redivo, D. d. A. Cabrini, J. d. F. G. Dias, M. D. Miguel, O. G. Miguel, J. M. d. Cunha, *Planta Medica.* **2019**, 85, 1216–1224.
21. C. R. Silva, L. M. Antunes, M. L. Bianchi, *Pharmacological Research.* **2001**, 43, 561–6.
22. H. Keita, C. B. R. d. Santos, M. M. Ramos, E. C. Padilha, R. B. Serafim, A. N. Castro, J. R. R. Amado, G. M. d. Silva, I. M. Ferreira, S. Giuliatti, J. C. T. Carvalho, *Journal of Biomolecular Structure and Dynamics.* **2021**, 39, 1017–1028.
23. A. T. Gasparin, E. S. Rosa, C. H. A. Jesus, I. C. Guiloski, H. C. d. S. de Assis, O. C. Beltrame, R. a. L. Dittrich, S. D. G. Pacheco, J. M. Zanoveli, J. M. d. Cunha, *Brain Research.* **2021**, 1767. DOI: 10.1016/j.brainres.2021.147557
24. J. Shin, M. H. Song, J. W. Oh, Y. S. Keum, R. K. Saini, *Antioxidants (Basel).* **2020**, 9, 532.
25. J. S. Park, B. D. Mathison, B. P. Chew, *Journal of Animal Science.* **2016**, 94, 135–43.
26. M. R. d. I. Vega, A. Krajisnik, D. D. Zhang, G. T. Wondrak, *Nutrients.* **2017**, 9, 1371.
27. I. Bereczki, H. Papp, A. Kuczmog, M. Madai, V. Nagy, A. Agócs, G. Batta, M. Milánkovits, E. Ostorházi, A. Mitrovi, J. Kos, Á. Zsigmond, I. Hajdú, Z. L'orincz, D. Bajusz, G. M. Keser u, J. Hodek, J. Weber, F. Jakab, P. Herczegh, A. Borbás, *Pharmaceuticals (Basel).* **2021**, 14, 1111.
28. S. Poornima, S. Jain, M. Shivashankar, *The Pharma Innovation Journal* **2019**, 8, 73.
29. P. R. Moreira, M. A. Maioli, H. CD Medeiros, M. Gueffi, F. TV Pereira2, F. E. Mingatto, *Biological Research.* **2014**, 47, 49.
30. A. D. P. Garcia, P. C. Vieira, C. C. Ribeiro, C. E. d. M. Jensen, L. S. Barcelos, M. E. Cortes, R. D. Sinisterra, *Journal of Biomedical materials Research Part B, Applied Biomaterials.* **2017**, 105, 1938–1949.
31. J. C. Vieira, M. C. C. Diniz, L. A. Mendes, R. D. S. Millán, G. D. Rodrigues, R. M. Orlando, C. C. Windmüller, *Environmental Nanotechnology, Monitoring & Management.* **2021**, 15, 100407.
32. R. G. d. O. Júnior, A. Bonnetta, E. Braconniera, H. Groulta, G. Pruniera, L. Beaugearda, R. Grougnetc, J. R. G. d. S. Almeida, C. A. A. Ferrazd, L. Picot, *Food and Chemical Toxicology.* **2019**, 125, 549–561.
33. <http://www.nbrienvic.nic.in/WriteReadData/CMS/Bixa%20orellana.pdf>.
34. D. d. A. Vilar, M. S. d. A. Vilar, T. F. A. d. L. e. Moura, F. N. Raffin, M. R. d. Oliveira, C. F. d. O. Franco, P. F. d. A. Filho, M. d. F. F. M. Diniz, J. M. B. Filho, *The Scientific World Journal.* **2014**, <http://dx.doi.org/10.1155/2014/857292>.
35. H. R. Chapman, S. Y. Thompson, H. M. Slade, *International Journal of Dairy Technology.* **1980**, 33, 162–164.
36. A. Häberli, H. Pfander, *Helvetica Chimica Acta.* **1999**, 82 (5), 696–706.
37. J. Rehbein, B. Dietrich, M. D. Grynbaum, P. Hentschel, K. Holtin, M. Kuehnle, P. Schuler, M. Bayer, K. Albert, *J. Sep. Sci.* **2007**, 30, 2382 – 2390.
38. B. Melka, D. Bisrat, N. Babu G., *J Pharmacovigil.* **2017**, 5 (4), DOI: 10.4172/2329-6887.1000237.
39. W. Rahmalia, J. F. Fabre, Z. Mouloungui, *Procedia Chemistry.* **2015**, 14, 455–464.